Dalton Transactions

Accepted Manuscript

ROYAL SOCIETY OF CHEMISTRY

www.rsc.org/dalton

The role of π-bonding on the high temperature structure of the double perovskites Ba_2CaUO_6 and $BaSrCaUO_6$.

Emily Reynolds[1], Gordon J. Thorogood[2], Maxim Avdeev[2], Helen E A Brand[3], Qinfen Gu[3] and Brendan J. Kennedy[1*]

1. School of Chemistry, The University of Sydney, Sydney, NSW 2006 Australia,
2. Bragg Institute and Institute for Materials Engineering, Australian Nuclear Science and Technology Organisation, Locked Bag 2001, Kirrawee DC NSW 2232,
3. Australian Synchrotron, 800 Blackburn Rd, Clayton, Victoria 3168, Australia.

Abstract

The high temperature structural behaviour of the uranium perovskites Ba_2CaUO_6 and $BaSrCaUO_6$ has been investigated using a combination of synchrotron X-Ray and neutron powder diffraction. Ba_2CaUO_6 undergoes a complex sequence of structures associated with the progressive loss of cooperative octahedral tilting: $P2_1/n \rightarrow I2/m \rightarrow I2/m \rightarrow I4/m \rightarrow Fm\bar{3}m$. The observation of the intermediate tetragonal structure, $I4/m$, in this, contrasts with the previously reported rhombohedral $R\bar{3}$ intermediate formed by the Ba_2SrUO_6 oxide. The importance of π-bonding in determining the structural sequence is discussed.

Introduction

Complex ceramics, such as perovskite oxides, have been proposed as stable hosts for high-level radioactive actinides waste forms. A critical requirement of these is their ability to retain the radioactive material whilst withstanding changes in temperature and composition induced by decay. Imitating geologically stable naturally occurring minerals, and incorporating actinides into a crystalline material, offers a durable alternative to the current solution of sequestration of high-level waste in borosilicate glass[1]. Strontium-90 is a high yield fission product and is a major constituent of high level waste, thus establishing the phases it forms with uranium, and the high temperature behaviour of these phases is relevant to the processing of spent nuclear fuel.

More generally, the determination and prediction of structure, and establishing relationship between the structure and physical properties is crucial in the optimisation of functional materials. Double perovskite oxides with the general formula $A_2BB'O_6$ have been the subject of recent studies and, in addition to their potential as waste forms, they have been shown to exhibit a range of interesting properties including superconductivity [2], ferromagnetism [3], magnetoresistance [4] and photoluminescence [5]. Perovskites are also currently gaining considerable attention for their leading performance in photovoltaic applications [6].

The $A_2BB'O_6$ double perovskite structure is derived from its parent ABO_3 structure by the, typically rock-salt like, ordered arrangement of two distinct *B* cations. This typically occurs if there is a sufficient difference in the size and/or charge of the *B* and *B*' cations. The double perovskite structure typically consists of ordered corner sharing BO_6 and $B'O_6$ octahedra with the larger *A* cations occupying the sites between.

The stability of the cubic perovskite structure can be estimated from the Goldschmidt tolerance factor [7] which is a measure of the size match of the *A* and *B* cations to the cubic perovskite topology. It is given by $t = (r_A + r_O)/[\sqrt{2}(r_B + r_o)]$ where r_A is the ionic radii of the 12 coordinate *A*-type cation, r_O the ionic radii of oxygen and r_B the average of the 6 coordinate ionic radii of the *B* and *B*' cations. If *t* is close to unity the structure is expected to be cubic, which for a double perovskite is in space group $Fm\bar{3}m$. A tolerance factor less than one describes the case where the *A* cation is too small for its cavity. This usually results in tilting of the BO_6 octahedra, in order to accommodate the bonding requirements of both cations, lowering the symmetry.[8]

Glazer developed a notation to describe octahedral tilting around the three orthogonal axes of the cubic perovskite structure [9]. Using these tilt systems, and taking into account the ordering of the two *B*-type cations, Woodward derived 13 possible space groups for double perovskites and, by surveying the literature, he established which of these were most common [10]. Howard *et al*. performed a group-theoretical analysis and established that one of the structures proposed by Woodward could not occur, but more importantly identified the group-subgroup relationships between the remaining 12 space groups [8]. This analysis revealed allowed phase-transition pathways. Howard's paper has served as a basis for identifying the structure of perovskites and, more importantly, of identifying possible intermediate phases that may form as a high symmetry perovskite transitions to its low symmetry structure, driven thermally, by the application of an external pressure, or by composition (sometimes referred to as chemical pressure). For double perovskites, the most commonly observed intermediate structures between a highly distorted monoclinic structure ($P2_1/n$) and the undistorted cubic ($Fm\bar{3}m$) are either tetragonal in space group $I4/m$ with an ($a^0a^0c^-$) tilt pattern or rhombohedral in $R\bar{3}$ ($a^-a^-a^-$).

Hindering the quest to discover why one intermediate is favoured over the other is the nontrivial task of differentiating between these tilt systems. Two major limitations in determining the correct structures of perovskites are instrument resolution and the presence of pseudo-symmetry. The effect of these, coupled with a reliance on X-ray diffraction methods, has resulted in many incorrect structures being described for perovskites. Establishing the correct symmetry of the material, and the nature of any thermally induced transitions is particularly relevant when studying materials involved in the nuclear fuel cycle, as thermal or radiation-induced first order phase transitions can result in micro-strains and defects which may lead to physical degradation of the waste form.

A recent study [11] of the high temperature behaviour of the double perovskite Ba_2SrUO_6 revealed that it undergoes the sequence of thermally induced phase transitions $P2_1/n \rightarrow R\bar{3} \rightarrow Fm\bar{3}m$. The room temperature structure of the related oxide $BaSrCaUO_6$ has, to our knowledge, only been previously described once, by Kemmler-Sack and Seeman [12], as cubic. Conversely Ba_2CaUO_6 was first described by Rudorff and Pfitzer [13] as cubic, then as orthorhombic [12], then as a slightly distorted cubic structure [14] and finally, more recently by Fu *et al.* [15], as monoclinic in $P2_1/n$.

Given the paucity of contemporary studies of temperature induced phase transitions in uranium oxides, the current study seeks to increase our knowledge through an investigation of the high temperature behaviour of the two closely related oxides, Ba_2CaUO_6 and $BaSrCaUO_6$, using a combination of synchrotron X-ray and neutron diffraction. Here we describe the thermally induced phase transition sequence followed by Ba_2CaUO_6 and $BaSrCaUO_6$ and compare these to the previously observed behaviour of Ba_2SrUO_6. These results are discussed in the context of current theories on the factors which stabilise the intermediate $I4/m$ or $R\bar{3}$ structure.

Experimental

Approximately 5g of Ba_2CaUO_6 and $BaSrCaUO_6$ were prepared by mixing stoichiometric amounts of U_3O_8, $BaCO_3$, $CaCO_3$ and $SrCO_3$ in an acetone slurry using an agate mortar and pestle. For Ba_2CaUO_6, the powder was pressed into a pellet and heated at 1000 °C for 12 h in air before being re-ground and sintered, again as a pellet, at 1100 °C for 12 h. For $BaSrCaUO_6$, the powder was heated at 800 °C for 12 h, then re-ground and pressed into a pellet and heated at 1000 °C for 12 h. The resulting yellow powder was again ground and pressed into a pellet before being sintered at 1195 °C.

Synchrotron X-ray powder diffraction data were collected using the powder diffractometer at BL-10 beamline of the Australian Synchrotron [16]. The samples were finely ground and housed in sealed 0.2 mm diameter quartz capillaries that were rotated during the measurements. The wavelength was set at ~ 0.826 Å and the precise value of this determined using a NIST LaB_6 standard reference material. Data were collected on heating from 25°C to 950°C and 1000°C, for Ba_2CaUO_6 and $BaSrCaUO_6$, respectively, using a Cyberstar hot-air blower. The structures were refined by the Rietveld method as implemented in the program RIETICA [17]. The peak shapes were modelled using a pseudo Voigt function and the background was estimated by interpolating between, up to, 40 selected points. The scale factor, detector zero point, lattice parameters, atomic coordinates and isotropic atomic displacement parameters were refined together with the peak profile parameters. An absorption correction was applied.

Neutron diffraction profiles were collected at ambient and high temperatures, upon heating up to 1000°C, using neutrons of wavelength 1.6215 Å on the high resolution powder diffractometer Echidna at ANSTO's OPAL facility [18]. Around 4 g of each sample were pressed into rods and sintered at their final heating temperatures for about 5 hrs before being placed into vanadium cans. The structures were obtained by performing refinements

simultaneously against the XRD and NPD data (where both data sets exist for the same temperature) using the Rietveld method as implemented in the program RIETICA [17]. The X-Ray histogram parameters were the same as described above, the peak shapes for the neutron histogram were also modelled using a pseudo Voigt function and the background was also estimated by interpolating between, up to, 40 selected points. The scale factor, detector zero point, lattice parameters, atomic coordinates and anisotropic atomic displacement parameters were refined together with the peak profile parameters.

Results

The room temperature Synchrotron X-ray and neutron powder diffraction patterns of $BaSrCaUO_6$ are shown in Figure 1. The synchrotron pattern is dominated by the primitive perovskite reflections, however we observe that these are split and that additional reflections are present. The intensity of the odd-odd-odd *R*-type reflections (**k** = ½, ½, ½) is contributed to by both anti-phase tilting of the BO_6 octahedra and *B*-site cation ordering. Substantial intensity in the $(111)_p$ reflection indicates an ordered arrangement of *B*-site cations, as expected, based on the size [19] and charge difference between Ca^{2+} (1.00 Å) and U^{6+} (0.73 Å). Although the splitting is quite small, examination of the symmetry-sensitive (*hhh*) and (*h*00) type reflections shows these are all clearly not single peaks and so the higher symmetry options of $Fm\bar{3}m$, $R\bar{3}$ and $I4/m$ can be eliminated. Consequently it is concluded that the cell is monoclinic. The presence of *M*-point reflections (**k** = ½, ½, 0) of the type even-even-odd, which arise from the in-phase (+*ve*) tilting of the octahedra, confirm $P2_1/n$ symmetry with the Glazer tilt system $a^-a^-c^+$. This structure is represented in figure 2. That the *M*-point reflections are very weak in the X-ray data is due to the relatively weak scattering power of oxygen in the presence of the heavier Ba, Sr, Ca and U cations. The observation of such peaks in the XRD pattern reflects the excellent signal-to-noise of the present data. The $P2_1/n$

space group is commonly observed in double perovskite oxides [8], and is also observed in Ba_2SrUO_6 at room temperature [11].

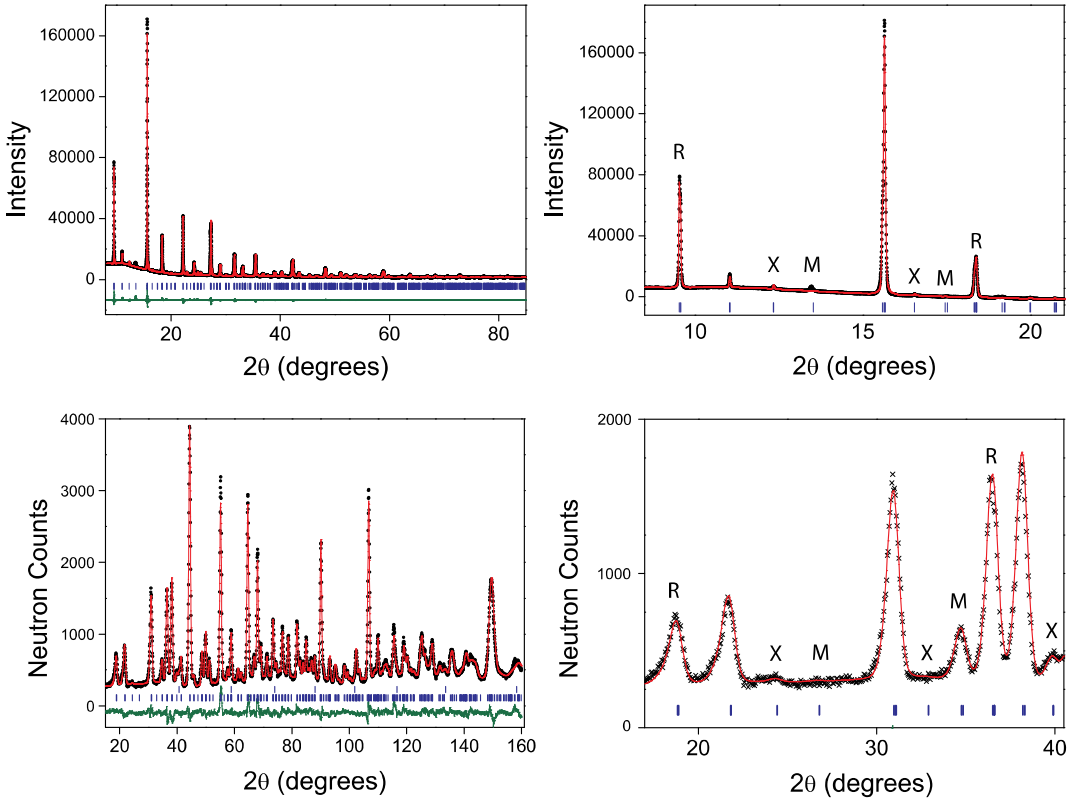

Figure 1. Room temperature S-XRD (top) and NPD (bottom) profiles for $BaSrCaUO_6$. The expanded angular range for both patterns shown on the right, highlights presence of selected *R*, *M* and *X*-point reflections. The observed and calculated data are represented by dots and a full line, respectively. The allowed Bragg reflections in $P2_1/n$ are indicated by tick marks, and the difference between the observed and calculated data is shown. The R_p and R_{wp} values are respectively 2.81% and 3.93% for S-XRD and 4.54% and 5.68% for NPD.

In the above discussion it was assumed that the Ba and Sr atoms are disordered on the *A*-site, and that the Ca and U atoms occupy the *B*-site in a fully ordered manner. These assumptions were tested by Rietveld refinement against the S-XRD data and found to be

valid. Ultimately the structure was refined using both S-XRD and the neutron diffraction data and the results are summarised in Table 1 and Table 2.

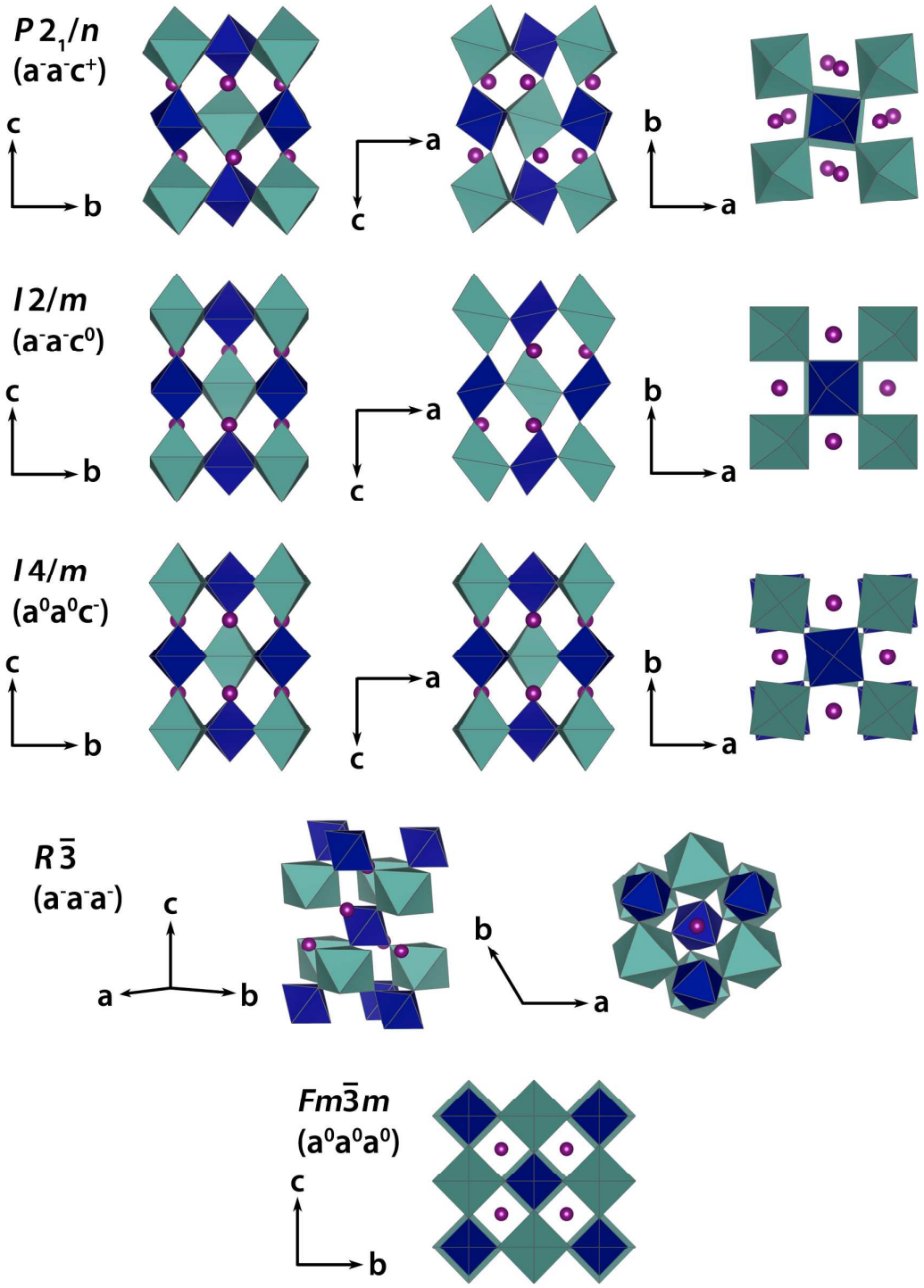

Figure 2. Representations of the commonly observed double perovskite tilt systems.

Table 1. Structural parameters obtained from the refinement against the combined S-XRD and NPD data of the double perovskites Ba_2CaUO_6 and $BaSrCaUO_6$ at ambient temperature.

	Ba_2CaUO_6	$BaSrCaUO_6$
Temp. (°C)	25	25
Space group	$P2_1/n$	$P2_1/n$
T	0.942	0.915
a (Å)	6.16170(4)	6.05541(7)
b (Å)	6.11787(4)	6.09083(6)
c (Å)	8.64588(5)	8.57261(9)
Vol (Å^3)	325.9192(8)	316.179(4)
β°	90.0984(3)	90.074(2)
Ba/Sr	4*e* (*x y z*)	4*e* (*x y z*)
x	-0.0028(2)	-0.0053(4)
y	0.4886(1)	0.4741(1)
z	0.2502(1)	0.2485(2)
B_{iso} (Å^2)	1.11(1)	1.60(1)
Ca	2*a* (0 0 0)	2*a* (0 0 0)
B_{iso}	0.59(3)	0.72(2)
U	2*b* (0 0 ½)	2*b* (0 0 ½)
B_{iso} (Å^2)	0.47(1)	0.64(1)
O1	4*e* (*x y z*)	4*e* (*x y z*)
x	0.0632(5)	0.0785(9)
y	0.0035(7)	0.0210(6)
z	0.2657(3)	0.2669(7)
B_{iso} (Å^2)	0.96(4)	1.53(10)
O2	4*e* (*x y z*)	4*e* (*x y z*)
x	0.2512(6)	0.2270(9)
y	0.2846(7)	0.3122(8)
z	-0.0321(7)	-0.0422(8)
B_{iso} (Å^2)	1.41(7)	1.52(10)
O3	4*e* (*x y z*)	4*e* (*x y z*)
x	0.2850(6)	0.2986(10)
y	0.7619(6)	0.7679(8)
z	-0.0370(7)	-0.0426(2)
B_{iso} (Å^2)	1.49(8)	1.60(1)
R_{wp} (SXRD)	3.42	4.19
R_p (SXRD)	2.63	3.06
R_{wp} (NPD)	6.99	7.69
R_p (NPD)	5.42	6.01

Table 2. Selected bond distances (Å) and angles (°) for Ba_2CaUO_6 and $BaSrCaUO_6$.

	Ba_2CaUO_6	$BaSrCaUO_6$
A-O1	2.990(4)	2.808(5)
-O1	3.186(4)	3.374(5)
-O1	2.721(3)	2.613(7)
-O2	2.918(4)	3.017(7)
-O2	3.178(4)	2.573(7)
-O2	2.788(4)	2.990(6)
-O3	2.961(5)	3.098(8)
-O3	2.711(4)	2.893(8)
-O3	3.143(5)	2.655(6)
Ca-O1	2.324(3)	2.353(6)
-O2	2.306(3)	2.341(5)
-O3	2.324(3)	2.358(5)
U-O1	2.067(3)	2.042(5)
-O2	2.085(4)	2.075(6)
-O3	2.089(3)	2.040(6)
Ca-O1-U	159.8(1)	154.4(3)
Ca-O2-U	162.8(2)	153.0(3)
Ca-O3-U	159.4(2)	154.8(3)

The structure of Ba_2CaUO_6 was also investigated using Synchrotron X-ray and neutron diffraction. Figure 3 shows the room temperature X-ray pattern for Ba_2CaUO_6 in which splitting of the $(444)_p$ into a triplet with intensity ratio 1:1:2, and of the $(400)_p$ into a doublet with intensity ratio 2:1, characteristic of a monoclinic cell, is observed. *M*-point reflections (of the type even-even-odd), which arise from the in-phase tilting, are only obvious in the neutron diffraction data (Fig. 3) and confirm $P2_1/n$ symmetry with tilt system $a^-a^-c^+$. The apparent absence of the *M*-point superlattice reflections in the S-XRD pattern can be explained by the relatively small average tilt angle, 5.39°, compared to 10.07° for $BaSrCaUO_6$. The refined structural parameters are in good agreement with the structure reported by Fu *et al.* who reported lattice parameters of a = 6.16146(7), b = 6.11877(7), c = 8.6975(1) Å, β = 90.1005(8) °.[15]

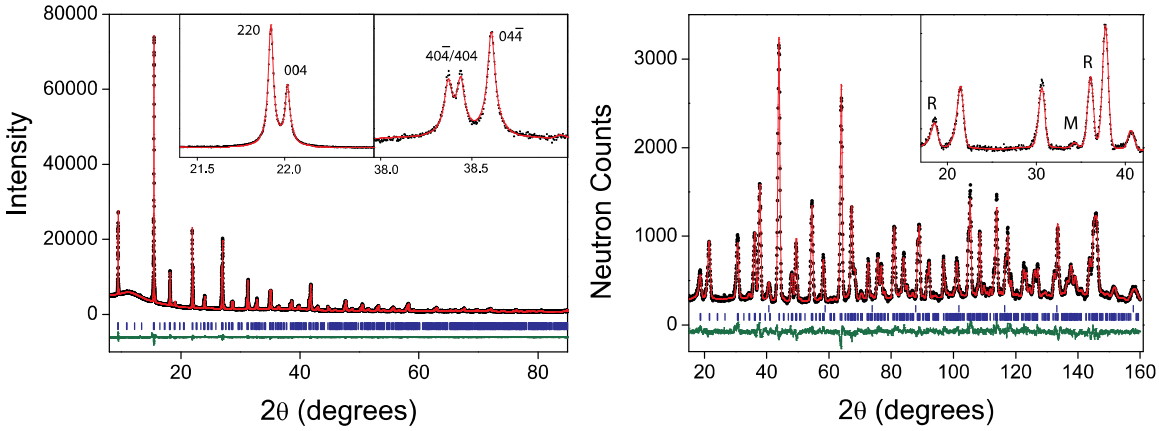

Figure 3. Left-hand panel shows the observed and calculated S-XRD profile for Ba_2CaUO_6 at room temperature. Insets show the $(400)_p$ and $(444)_p$ reflections, with splitting characteristic of a monoclinic cell. The right panel shows observed and calculated NPD profile for Ba_2CaUO_6 at room temperature, the inset highlights the *M*-point reflection.

Variable temperature X-ray and neutron diffraction studies of both compounds were performed, and revealed that $BaSrCaUO_6$ remains monoclinic with $P2_1/n$ symmetry up to 1000 °C, as demonstrated by the persistence of the *M*-point reflections in the S-XRD pattern (Fig 4). The unit cell parameters showed unexceptional thermal expansion behaviour and there was no indication for discontinuity (Fig 4). The monoclinic β angle was approximately independent of temperature until around 800 °C, above which it began to decrease; evidently a continuous transition to a higher symmetry structure will only occur at still higher temperatures.

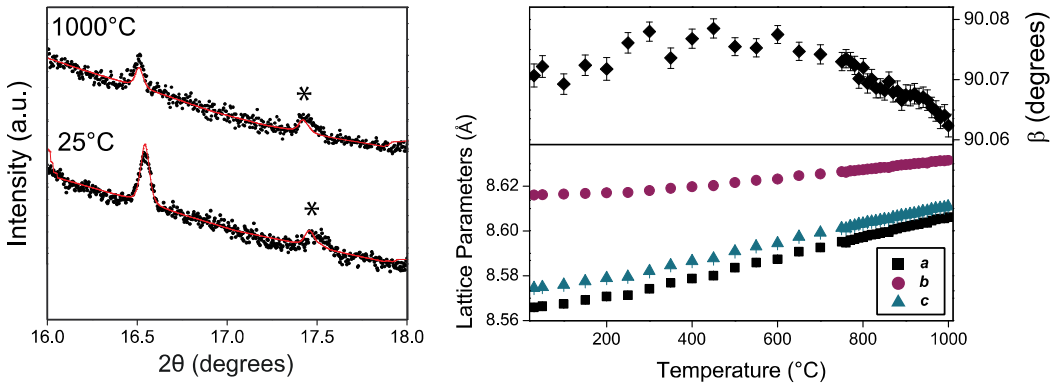

Figure 4. Left image shows Rietveld refinements of S-XRD profiles of $BaSrCaUO_6$ at 25 °C and 1000 °C, showing the presence of the M-point reflection indicated (*) at high temperatures, which indicates that the structure remains monoclinic in $P2_1/n$. Right hand image shows monoclinic angle β and reduced lattice parameters extracted from Rietveld refinements of variable temperature S-XRD data.

As noted above, the *M*-point reflections for Ba_2CaUO_6 are too weak to be observed in the S-XRD data, although these are present in the neutron data measured at room temperature. The NPD pattern of Ba_2CaUO_6 measured at 300 °C showed no evidence for any M-point reflections, indicating the loss of the in-phase octahedral tilting before this temperature. Due to limited instrument availability, neutron diffraction data were not collected between 25 and 300 °C. The splitting of the Bragg reflections, $(400)_p$ and $(444)_p$, in the S-XRD patterns indicates that the structure remains monoclinic at 300 °C, and the monoclinic space group $I2/m$ ($a^-a^-c^0$) with no in-phase tilt is a likely candidate.[8]

Despite the lack of neutron data between 25 and 300 °C, and the absence of observable intensity in the *M*-point reflections in the S-XRD patterns, it is possible to estimate the temperature at which the transition from $P2_1/n$ occurs, as about 150 °C, by the change in the thermal expansion of the lattice parameters obtained from Rietveld refinements against the S-XRD data (Fig 5). A similar change occurred for the analogous *Pbnm* ($a^-a^-c^+$) to *Imma* ($a^-a^-c^0$) transition in $SrTcO_3$ [20]. The transition between the $P2_1/n$ - $I2/m$ monoclinic structures in Ba_2CaUO_6 appears to be continuous. This transition has been observed in

similar systems such as Sr_2YTaO_6 [21] and according to Howards group-subgroup relationship diagram [8], is allowed to be continuous. Rietveld refinements using the *I*2/*m* model provided an acceptable fit to the S-XRD data above 150 °C.

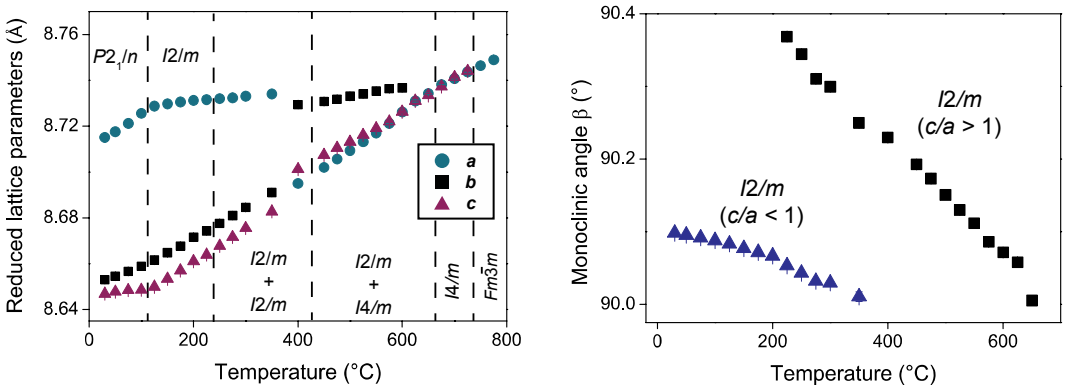

Figure 5. Lattice parameters extracted from Rietveld refinements of S-XRD and combined NPD and S-XRD data of Ba_2CaUO_6 as a function of temperature. Only the lattice parameters of the dominant phase in the two phase regions are shown, for clarity. Right hand panel shows monoclinic angles for the $P2_1/n$, and both *I*2/*m* phases.

Attempts to use this model to fit the S-XRD data measured at temperatures above 225 °C and the neutron diffraction data at 300 °C were unsuccessful, acceptable calculated intensities could not be achieved Likewise, single phase models in higher symmetries were also unsuccessful (Fig 6). The excellent fits obtained at room temperature and high temperature (above 700 °C) to single phase models, confirm that this is not a result of poor sample quality and suggest the possibility that two or more phases were co-existing. Ultimately, the only model that provided an acceptable fit to the data in the temperature range 225 – 425 °C was a two-phase *I*2/*m* + *I*2/*m* model, where the second *I*2/*m* phase has $c/a > 1$, as opposed to the first which has $c/a < 1$. The transition between two forms of *I*2/*m* must be first order, and so the presence of a two-phase region is not unexpected.

This curious phenomenon involving the reversal of the *c*/*a* ratio has been observed in other systems including $SrZrO_3$[22] during the transition from *Imma* to *I*4/*mcm*, as well as in Ba_2NdNbO_6 and Ba_2NdTaO_6 [23] during the *I*2/*m* to *I*4/*m* transition and is considered to be a consequence of the re-orientation of the tilts. It was recently argued [24] that for *I*2/*m* with the $a^-a^-c^0$ tilt system the *a*-axis should be slightly longer than the *b*-axis, and this is observed for most Ba-containing double perovskites, as well as in the $P2_1/n$ and first *I*2/*m* structures of Ba_2CaUO_6. The S-XRD data provides no evidence for anti-site disorder, and it is difficult to understand how such disorder would impact on the relative magnitude of the unit cell parameters. The origin of the reversal of the *c*/*a* ratio is unknown.

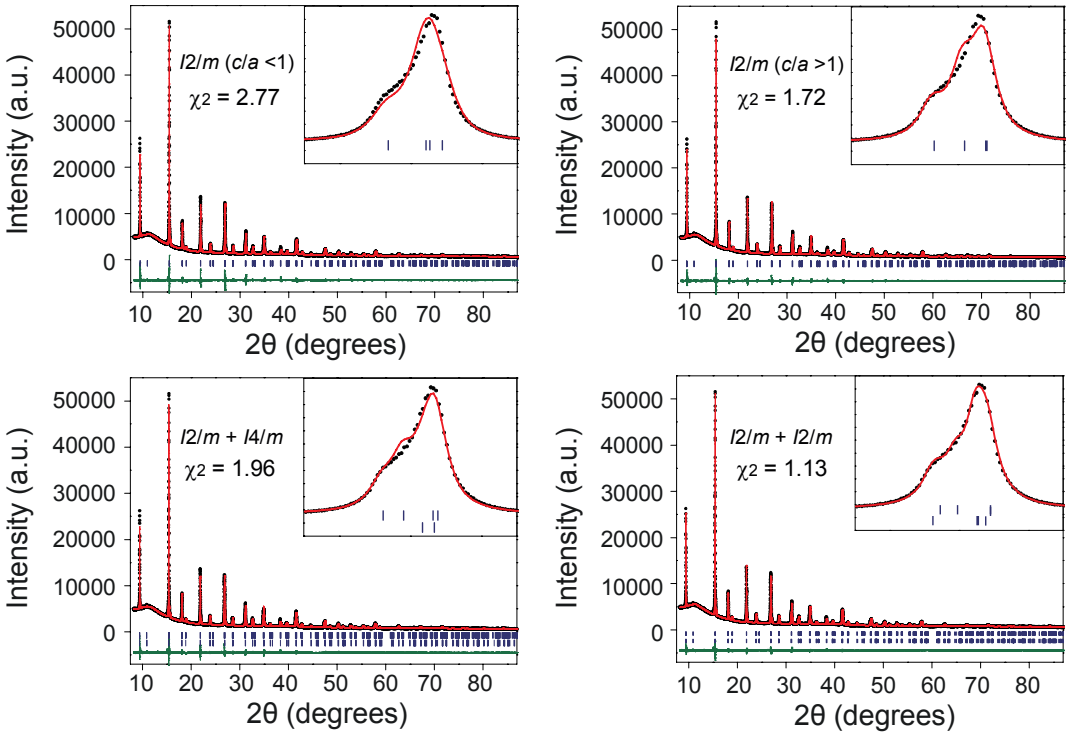

Figure 6. Rietveld refinement profiles of S-XRD data of Ba_2CaUO_6 using different models. The insets show the fit to the most intense reflection $(220)_p$ at around 2θ=15°.

The possible pathways that a monoclinic structure can take to cubic are outlined in Howards group-subgroup relationship diagram [8]. Typically the structure will reach the cubic

via either a tetragonal $I4/m$ or rhombohedral $R\bar{3}$ intermediate. Distinguishing between these possibilities can be challenging given a highly pseudo-symmetric structure. Usually this is done by examining the (*hhh*) and (*h*00) type reflections which are single and double, respectively, in $I4/m$ and the opposite in $R\bar{3}$. However, at 700 °C both of these reflections are single, due to pseudo-symmetry. Examining the temperature dependence of the full-width at half maximum (FWHM) of selected reflections, including the $(004)_p$ and $(444)_p$, suggests that the transition to cubic occurs near, the FWHM values for the $(004)_p$ and $(444)_p$ being 0.0329° and 0.0467°, respectively at 72 5°C.

Since the splitting of the diagnostic reflections is insufficient to allow us to differentiate between the possible structures, we depend on the neutron data to establish the appropriate structures at high temperatures. The NPD pattern measured at 600 °C could be adequately fitted in the tetragonal space group $I4/m$ but not in the rhombohedral space group $R\bar{3}$. A two phase $I2/m$ and $I4/m$ model was required to fit the data between 450 °C and 650°C. Howard [22 23] showed that a $I2/m$ ($a^-a^-c^0$) to $I4/m$ ($a^0a^0c^-$) transition must be discontinuous, since the transition involves the rearrangement of tilts from about the *a* and *b* axes to around the *c* axis and this allows the possibility of phase co-existence as has been observed in other double perovskites [25, 26]. Above 650°C, where the $(444)_p$ reflection is observed as a single peak the data were reproduced by a single phase $I4/m$ tetragonal model. By examination of the FWHM of the $(004)_p$ and $(444)_p$ reflections we can estimate the temperature at which the structure transforms to cubic is around 725 °C, and Rietveld refinements using a cubic $Fm\bar{3}m$ model above this temperature were successful. This $I4/m$ to $Fm\bar{3}m$ transition, as expected, appears to be continuous. The lattice parameters extracted from the refinements using the structures described above, as well as the monoclinic angle for both $I2/m$ phases are shown in figure 5.

Discussion

The tolerance factors of Ba_2CaUO_6 and $BaSrCaUO_6$, 0.942 and 0.915 respectively, suggest that the latter structure will be more distorted than the former due to the presence of the smaller Sr cation in the *A*-site. The average Ca-O-U bond angles (161° for Ba_2CaUO_6 and 154° for $BaSrCaUO_6$) and the observed tilt angles (5.39° for Ba_2CaUO_6 and 10.07° for $BaSrCaUO_6$) calculated using TUBERS [27] demonstrate this to be the case. The average *A*-site (Ba^{2+}/Sr^{2+})-O bond distances are appreciably shorter in $BaSrCaUO_6$ (2.744 Å) than in Ba_2CaUO_6 (2.851 Å), reflecting with the presence of the smaller Sr^{2+} cation on the *A*-site. The average U^{6+}-O bond distances are very similar, 2.052 Å and 2.058 Å for Ba_2CaUO_6 and $BaSrCaUO_6$, respectively, however the average Ca^{2+}-O distance is somewhat longer in $BaSrCaUO_6$ (2.348 Å) than in Ba_2CaUO_6 (2.316 Å). This is a consequence of the relatively short *A*-O bonds when Sr^{2+} is in the *A*-site. Bond valence sum (BVS) calculations of the room temperature structures show the Ca^{2+} cation is relatively more stable in $BaSrCaUO_6$ than in Ba_2CaUO_6, with the BVS values being 2.15 and 2.33, respectively.

The BVS calculations show both the U^{6+} and Ca^{2+} to be relatively stable in $BaSrCaUO_6$ at high temperatures, with BVS between 6.1-6.3 and 2.1-2.3, respectively. In Ba_2CaUO_6, the U^{6+} is somewhat over-bonded in the *I*2/*m* phase with $c/a < 1$ (BVS = 6.16), and under-bonded (5.08) in the second *I*2/*m* phase that forms with $c/a > 1$. It should be noted that room temperature values for R_0 were used in all calculations, and that although this impacts the absolute values of high temperature BVS, the relative values are still useful.

Comparing the tolerance factors and transition temperatures of the two perovskites with that previously reported for Ba_2SrUO_6, the stability of the tilted structures in $BaSrCaUO_6$ is unexpected. A lower tolerance factor indicates a more distorted structure, and structures that are relatively more distorted have been shown to have higher transition

temperatures.[25, 28] Based on the calculated tolerance factors Ba_2SrUO_6 is expected to adopt are more distorted structure since this has the lowest tolerance factor (t = 0.905). Consequently any transition to a higher symmetry structure should occur at a higher temperature than in $BaSrCaUO_6$ which has the higher tolerance factor. This expectation is not met; the structure of $BaSrCaUO_6$ remains monoclinic in $P2_1/n$ to above 1000 °C whereas Ba_2SrUO_6 transforms from $P2_1/n$ to $R\bar{3}$ at 630 °C and cubic near 930 °C. It is possible that the mixed *A*-site creates flexibility around the *B*-sites and allows the structure to more easily satisfy bonding requirements, thus stabilising the distorted structure. This is reflected in the bond valence sums which show the Ca and U to be stable in their sites up to high temperatures in the $BaSrCaUO_6$ compound. Whilst appealing this suggestion is not supported by experimental studies of other $A_2BB'O_6$ double perovskites including $Ca_{2-x}Sr_xNiWO_6$ and $Ba_{2-x}Sr_xNiWO_6$ [25] where the temperature at which a transition to a higher symmetry structure occurs reflects the tolerance factor.

A second unusual feature of the present uranium oxides is the observed $I2/m$-$I2/m$ transition in Ba_2CaUO_6 that involves a reversal of the c/a ratio. To our knowledge this is a unique example of such a transition within the same space group and it is not predicted by Howard's group theory analysis. In other examples where Howard's group theory is apparently violated, secondary effects such as valence transition in $Sr_{1-x}Ce_xMnO_3$ [29] and $SrLaCoIrO_6$ [30] are present. It is not obvious what electronic effects would be present in Ba_2CaUO_6. BVS calculations suggest the transition reduces the over-bonding of the $c/a < 1$ $I2/m$ phase. In general when the over-bonding of the *B*-site cation becomes unstable, the structure rearranges to re-optimise the bonding, in either a first order (e.g. $I2/m$-$I4/m$) or continuous ($I4/m$-$Fm\bar{3}m$) fashion. We postulate that the system encounters an energetic barrier that inhibits the $I2/m$-$I4/m$ transition, and that the second $I2/m$ phase with $c/a > 1$ is essentially the kinetic product of the thermodynamic barrier, in which the axes have reversed

but the tilt system has not yet changed. A computational investigation would be required to confirm this explanation.

It is interesting to compare the present results with those of Ba_2SrUO_6 since these adopt different intermediate structures, $I4/m$ and $R\bar{3}$, for Ba_2CaUO_6 and Ba_2SrUO_6, respectively. The same situation occurs in the analogous Ba_2CaWO_6 and Ba_2SrWO_6 perovskites; Fu and co-workers [15] found that Ba_2CaWO_6 adopts the $I4/m$ structure below 240 K, whereas Ba_2SrWO_6 adopts the $R\bar{3}$ structure above about 600 K, the different temperatures reflect the different tolerance factors. Evidently the precise nature of the octahedral *B*-site cation (Ca vs Sr) is important in favouring the tetragonal or rhombohedral intermediate structure.

The present A_2BUO_6 oxides are part of a wider family of double perovskites where a divalent alkaline earth cation occupies on octahedral site and a hexavalent cation the other. The three oxides $Ba_2SrM^{6+}O_6$, M = W, Mo and Te all adopt the $R\bar{3}$ structure, either at room temperature or upon heating [15]. The analogous Ca compounds are all cubic at room temperature, and to our knowledge only Ba_2CaWO_6 has been studied at low temperatures, and this transforms to the tetragonal $I4/m$ structure upon cooling. The tetragonal structure is also observed in $BaSrCaWO_6$ and Sr_2CaWO_6 (above 860 °C) that also contain Ca^{2+} on the octahedral site [31]. Variable temperature studies of the other compounds would be useful to determine if they also adopt the $I4/m$ symmetry.

It is tempting to generalise that when Sr occupies the B-site the rhombohedral structure is favoured over the tetragonal structure and that for Ca on the B-site the reverse is true. The sensitivity of the structure to this is evident in $Ba_2Ca_{0.75}Sr_{0.25}WO_6$ where the addition of a small amount of strontium onto the *B*-site results in the formation of the rhombohedral phase [31].

Fu *et al.* attempted to explain why a particular double perovskite structure favours the tertragonal or rhombohedral intermediate using Woodwards' analysis of ABO_3 perovskites[32]. Woodward showed that the rhombohedral tilt system results in the highest coulombic attraction between ions, so when an *A*-cation is highly charged with small to moderate tilting angles (i.e. TF close to 1) the rhombohedral structure will be stabilised because the attractive term overweighs the repulsive term. Fu *et al.* asserted that the nature of the *B*-O bonding must also play a role, and suggested that the increase in covalence of the *B*-O bond favours the coordination sphere of oxygens around the *A*-cation that maximises coulomb attraction. Since the oxygen anions around the *A*-cation are coplanar in the $R\bar{3}$ tilt system (as opposed to $I4/m$) this increases the number of *A*-cation orbitals involved in the bonding and thus maximises the coulombic attraction. Therefore, a more covalent *B*-O bonding interaction stabilizes the rhombohedral symmetry[31].

The covalence of a bond can be evaluated using Paulings' electronegativity scale [33], with more similar electronegativity values resulting in a more covalent bond. The electronegativity (χ) of oxygen is 3.5 and that for strontium and calcium, 0.95 and 1.00, respectively. Given this relatively small difference in electronegativity between strontium and calcium, it would be surprising if this was a dominant factor in differentiating between $I4/m$ and $R\bar{3}$.

Saines *et al*. acknowledged the significance of the octahedral cation but they argued that the π-bonding between the octahedral cation and the oxygen plays a vital role in determining the symmetry[23]. For *B* cations capable of π-bonding, the tetragonal symmetry will be favoured as 1/3 of the *B*-O-*B*' angles are 180°, whereas none are in $R\bar{3}$. This explanation appears valid in the uranium perovskites. Both Sr^{2+} and Ca^{2+} have empty *d*-

orbitals and are capable of π-bonding, but the smaller 3*d* Ca^{2+} will have stronger π-bonding than the larger diffuse 4*d* Sr^{2+}, favouring the tetragonal structure when Ca is in the *B*-site.

Conclusion

The high temperature behaviour of the double perovskites Ba_2CaUO_6 and $BaSrCaUO_6$ has been investigated with $BaSrCaUO_6$ retaining the monoclinic $P2_1/n$ structure up to 1000 °C. Rietveld analysis on a combination of synchrotron X-Ray and neutron diffraction data revealed that upon heating, Ba_2CaUO_6 undergoes the series of phase transitions $P2_1/n \rightarrow I2/m \rightarrow I2/m \rightarrow I4/m \rightarrow Fm\bar{3}m$. A surprising observation was the formation of a second $I2/m$ phase with reversed c/a axis ratio at elevated temperatures 650 °C. To our knowledge, a $I2/m$ to $I2/m$ transition of this nature has not before been reported in double perovskites. The observation of the intermediate tetragonal structure, $I4/m$, in this contrasts with the previously reported rhombohedral $R\bar{3}$ intermediate formed by the Ba_2SrUO_6 oxide. Comparing these with other $Ba_2M'M^{6+}O_6$ systems, with M' = Sr or Ca, the intermediate structure in each known case is $I4/m$ and $R\bar{3}$ for the Ca and Sr oxides, respectively. These results are consistent with π-bonding being a dominant factor in determining the intermediate structure.

Acknowledgments

We acknowledge the Australian Research Council and the Australian Institute of Nuclear Science and Engineering for support of this work which was, in part, performed at the Powder Diffraction beamline at the Australian Synchrotron.

References

1. R. C. Ewing, *Proceedings of the National Academy of Sciences of the United States of America*, 1999, 96, 3432-3439.
2. M. L. Norton and H. Y. Tang, *Chemistry of Materials*, 1991, 3, 431-434.
3. M. Azuma, K. Takata, T. Saito, S. Ishiwata, Y. Shimakawa and M. Takano, *Journal of the American Chemical Society*, 2005, 127, 8889-8892.
4. K. L. Kobayashi, T. Kimura, H. Sawada, K. Terakura and Y. Tokura, *Nature*, 1998, 395, 677-680.
5. S. Ye, C. H. Wang, Z. S. Liu, J. Lu and X. P. Jing, *Applied Physics B-Lasers and Optics*, 2008, 91, 551-557.
6. M. Graetzel, *Nature Materials*, 2014, 13, 838-842.
7. V. M. Goldschmidt, *Naturwissenschaften*, 1926, 14, 477-485.
8. C. J. Howard, B. J. Kennedy and P. M. Woodward, *Acta Crystallographica Section B-Structural Science*, 2003, 59, 463-471.
9. A. M. Glazer, *Acta Crystallographica Section A*, 1975, 31, 756-762.
10. P. M. Woodward, *Acta Crystallographica Section B-Structural Science*, 1997, 53, 32-43.
11. E. Reynolds, B. J. Kennedy, G. J. Thorogood, D. J. Gregg and J. A. Kimpton, *Journal of Nuclear Materials*, 2013, 433, 37-40.
12. S. Kemmlersack and I. Seemann, *Zeitschrift Fur Anorganische Und Allgemeine Chemie*, 1975, 411, 61-78.
13. W. Rudorff and F. Pfitzer, *Zeitschrift Fur Naturforschung Section B-a Journal of Chemical Sciences*, 1954, 9, 568-569.
14. R. Gens, J. Fuger, L. R. Morss and C. W. Williams, *Journal of Chemical Thermodynamics*, 1985, 17, 561-573.
15. W. T. Fu, Y. S. Au, S. Akerboom and D. J. W. Ijdo, *Journal of Solid State Chemistry*, 2008, 181, 2523-2529.
16. K. S. Wallwork, B. J. Kennedy and D. Wang, *AIP Conference Proceedings*, 2007, 879, 879-882.
17. B. A. Hunter and C. J. Howard, *RIETICA A Computer Program for Rietveld Analysis of X-Ray and Neutron Powder Diffraction Patterns*, 1998, , .
18. K.-D. Liss, B. Hunter, M. Hagen, T. Noakes and S. Kennedy, *Physica B-Condensed Matter*, 2006, 385-86, 1010-1012.
19. R. Shannon, *Acta Crystallographica Section A*, 1976, 32, 751-767.
20. G. J. Thorogood, M. Avdeev, M. L. Carter, B. J. Kennedy, J. Ting and K. S. Wallwork, *Dalton Transactions*, 2011, 40, 7228-7233.
21. Q. Zhou, B. J. Kennedy and M. Avdeev, *Journal of Solid State Chemistry*, 2010, 183, 1741-1746.
22. C. J. Howard, K. S. Knight, B. J. Kennedy and E. H. Kisi, *Journal of Physics-Condensed Matter*, 2000, 12, L677-L683.
23. P. J. Saines, J. R. Spencer, B. J. Kennedy, Y. Kubota, C. Minakata, H. Hano, K. Kato and M. Takata, *Journal of Solid State Chemistry*, 2007, 180, 3001-3007.
24. W. T. Fu, R. J. Gotz and D. J. W. Ijdo, *Journal of Solid State Chemistry*, 2010, 183, 419-424.
25. Q. D. Zhou, B. J. Kennedy, C. J. Howard, M. M. Elcombe and A. J. Studer, *Chemistry of Materials*, 2005, 17, 5357-5365.
26. P. J. Saines, B. J. Kennedy and M. M. Elcombe, *Journal of Solid State Chemistry*, 2007, 180, 401-409.
27. M. W. Lufaso and P. M. Woodward, *Acta Crystallographica Section B-Structural Science*, 2001, 57, 725-738.
28. Q. D. Zhou, B. J. Kennedy and M. M. Elcombe, *Journal of Solid State Chemistry*, 2007, 180, 541-548.

29. B. J. Kennedy, P. J. Saines, Q. D. Zhou, Z. M. Zhang, M. Matsuda and M. Miyake, *Journal of Solid State Chemistry*, 2008, 181, 2639-2645.
30. N. Narayanan, D. Mikhailova, A. Senyshyn, D. M. Trots, R. Laskowski, P. Blaha, K. Schwarz, H. Fuess and H. Ehrenberg, *Physical Review B*, 2010, 82, 024403.
31. W. T. Fu, S. Akerboom and D. J. W. Ijdo, *Journal of Solid State Chemistry*, 2007, 180, 1547-1552.
32. P. M. Woodward, *Acta Crystallographica Section B-Structural Science*, 1997, 53, 44-66.
33. L. Pauling, *Journal of the American Chemical Society*, 1932, 54, 3570-3582.

Table of Content Figure

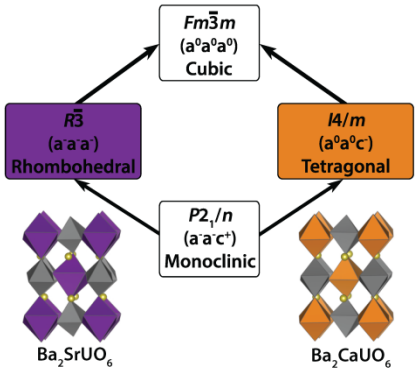

Synopsis: The structure of the uranium perovskites Ba_2CaUO_6 and $BaSrCaUO_6$ have been determined using a combination of synchrotron X-Ray and neutron diffraction powder diffraction. Ba_2CaUO_6 undergoes a complex sequence of structures associated with the progressive loss of cooperative octahedral tilting. That this forms a tetragonal intermediate demonstrates the importance of π-bonding in these oxides.